Exp Brain Res (1996) 110:1–14

RESEARCH ARTICLE

S.J. Heinen · E.L. Keller

The function of the cerebellar uvula in monkey during optokinetic and pursuit eye movements: single-unit responses and lesion effects

Received: 11 April 1995 / Accepted: 18 January 1996

Abstract The cerebellum is known to participate in visually guided eye movements. The cerebellar uvula receives projections from pontine nuclei that have been implicated in visual motion processing and the generation of smooth pursuit. Single-unit and lesion studies were conducted to determine how the uvula might further process these input signals. Purkinje cells and input fibers were recorded during a variety of visual and oculomotor paradigms. Most Purkinje cells were modulated in either an excitatory or inhibitory fashion by prolonged, horizontal optokinetic drum rotation. A small proportion of cells responded during smooth tracking of a small spot of light. As a paradox to the physiological data, lesions of the uvula produced a profound effect on smooth-pursuit eye movements. Initial eye velocity for pursuit in the direction contraversive to the lesion site was increased substantially following lesions in comparison with prelesion controls. The lesions also affected optokinetic nystagmus in the direction contraversive to the lesion, but not as drastically as they did pursuit. Overall the results suggest that the uvula is not in the neuronal pathway that directly controls pursuit, but instead serves to adjust the gain of this system as a result of abnormal periods of motion of the visual world.

Key words Smooth pursuit · Optokinetic nystagmus · Single neurons · Lesion · Cerebellum · Monkey

Introduction

The cerebellar cortex is involved in generating most types of eye movements. In particular, among the cortical regions, the flocculus/ventral paraflocculus and the middle vermis (lobules VI and VII) seem to be the most heavily involved (see Keller 1988; Miles 1991 for reviews). Neurons in both areas code aspects of visual and motor signals used for smooth-pursuit eye movement control (e.g., Büttner and Waespe 1984; Lisberger and Fuchs 1978; Miles et al. 1980; Noda and Suzuki 1979; Stone and Lisberger 1990; Suzuki and Keller 1988a, 1988b), and lesions in either area create pursuit deficits (Zee 1982; Keller 1988). The middle vermis also participates in saccade generation (Kase et al. 1980; McElligott and Keller 1982; Noda and Fujikado 1987; Ohtsuka and Noda 1991), and the flocculus/ventral paraflocculus is involved in the vestibulo-ocular reflex (VOR) and optokinetic nystagmus (OKN; Büttner and Waespe 1981; Miles and Fuller 1975; Lisberger and Fuchs 1978). Both the middle vermis (lobules VI and VII) and the flocculus receive projections from the nucleus reticularis tegmenti pontis (NRTP; Brodal 1979) and from the pontine nuclei (Brodal 1982; Langer et al. 1985) (but see Glickstein et al. 1994 for evidence that the flocculus does not receive inputs from the pontine nuclei). These are brainstem regions where cells respond to moving visual stimuli and during smooth eye movements (Keller and Crandall 1983; Crandall and Keller 1985; Mustari et al. 1988; Thier et al. 1988; Suzuki et al. 1990).

In the primate, the uvula (lobule IX of the cerebellar vermis) receives at least as strong an input from visual areas of the pontine nuclei as do the middle vermis and the flocculus (Brodal 1982; Glickstein et al. 1994). Visual projections to the uvula arise predominately from the dorsolateral and medial parts of the dorsal pontine nuclei (Brodal 1982; Glickstein et al. 1994). The projections favor the dorsal folia a and b of the uvula, but extend into folia c of the ventral uvula. Projections from oculomotor-related portions of the vestibular nuclei have been reported to be more abundant to the uvula than to the middle vermis (Brodal and Brodal 1985). Purkinje cells in the uvula then project to the caudal portion of the fastigial nucleus (FN) and the vestibular nuclei (Angaut and Brodal 1967; Voogd and Bigaré 1980), both areas implicated in pursuit control (Keller and Heinen 1991). The uvula projects for the most part to nonoculomotor portions of the vestibular nuclei, but there are sparse connections to the superior and lateral vestibular nuclei, re-

S.J. Heinen (✉) · E.L. Keller
The Smith-Kettlewell Eye Research Institute,
2232 Webster Street, San Francisco, CA 94115, USA;
Fax: +1-415-561-1610, e-mail: heinen@skivs.ski.org

gions which have been associated with oculomotor function. The projections from the uvular cortex follow the zonal projection pattern established for other cerebellar cortical areas (see Voogd and Bigaré 1980 for reviews). Zone A, the most medial vermal zone, projects to the FN, while the more lateral zone B projects to the vestibular nucleus and the most lateral extent of zone B projects to the posterior nucleus interpositus. Sparse projections to the nucleus prepositus hypoglossi have also been reported (Angaut and Brodal 1967). Therefore it seemed likely that the uvula would also participate in the generation of visually guided eye movements. No previous single-unit studies have assessed uvular involvement in smooth tracking or saccades; however, there has been work done on neural correlates of visual surround motion in the rabbit uvula (Precht et al. 1976). Furthermore, combined lesions of the nodulus and uvula have resulted in an inability of monkeys to suppress or "dump" optokinetic afternystagmus (OKAN) by visual stimulation (Waespe et al. 1985).

We set out to determine whether the uvula plays a role in the generation of visually guided eye movements using behavioral paradigms, single-unit recording and lesion techniques that have been used to clarify the oculomotor functions of the flocculus/ventral paraflocculus and middle vermis. Our results were very different from those reported for the other two cerebellar oculomotor areas. Very few cells in the uvula were active during smooth pursuit or saccades. Instead, most uvular cells were modulated in a directionally selective manner after long latencies by prolonged optokinetic stimulation. Paradoxically, lesions to the uvula predominately affected pursuit and the initial phase of OKN. The results suggest that the uvula is not in the pursuit pathway that the middle vermis and the flocculus/ventral paraflocculus are thought to subserve, but instead has a modulatory effect on the gain of pathways that produce smooth eye movements. Descriptions of this research have appeared previously in a shorter form (Heinen and Keller 1992).

Materials and methods

Preparation

Three monkeys (*Macaca fascicularis*) were used in the study. Each animal was implanted with a coil of Teflon-coated stainless steel wire mounted under the conjunctiva of one eye to record eye movements. A stainless steel chamber (16 mm diameter) was stereotaxically positioned on the skull with a posterior angle of 10° to allow single-unit recording from the cerebellar uvula, and two transverse stainless steel tubes were mounted on the skull to immobilize the head. Both devices were fixed in place with dental acrylic cement. All surgeries were performed under sterile conditions with deep anesthesia (pentobarbital sodium 25 mg/kg i.v.). Animals were initially anesthetized for intravenous catheterization with ketamine (20 mg/kg i.m.) and given atropine sulfate (0.05 mg/kg i.m.) to suppress salivation 30 min before ketamine injection. Sutured incisions were treated with antibiotic ointments, and penicillin was administered during the postsurgical recovery period. The analgesic torbutrol was given (0.05 mg/kg i.m.) to alleviate postsurgical discomfort. Following recovery from surgery, the monkeys were taken to the recording room on a daily basis, for sessions lasting several hours, to collect experimental data. For 5 successive days each week, the animals received all of their water during recording sessions. The recording periods were separated by 2 days of ad lib water. All experimental protocols were approved by the Institutional Animal Care and Use Committee at the California Pacific Medical Center and complied with the guidelines of the Public Health Service policy on the humane care and use of laboratory animals.

Unit recording

Tungsten microelectrodes insulated with Isonel-31 were lowered within a stainless steel hypodermic guide tube to a point just below the cerebellar tentorium and then were hydraulically advanced from the tip of the guide tube through the cerebellum. Since the chamber was located over the midline with a 10° posterior angle of inclination, most microelectrode recording penetrations passed through lobules VI and VII of the middle vermis before reaching the uvula. The characteristic "swishing" sound of neurons in this area during saccadic eye movements was monitored through an auditory speaker and served as a landmark to help us locate the uvula.

Our classification of unitary potentials in the uvula follows closely that already established in the flocculus and the middle vermis (Miles et al. 1980; Suzuki and Keller 1988a). Purkinje cell (P-cell) activity was identified by the presence of the very low frequency "complex spikes" interspersed among "simple spikes." Simple spike activity of identified P cells always had a high-frequency, irregular background rate, even in the absence of any intended stimulation. We also recorded from a few units that showed the same irregular, high-frequency discharge characteristics as identified P-cells, but from which we were unable to detect the presence of a complex spike. Cells of this type were usually recorded from layers in the cerebellar cortex where identified P-cells were recorded and had response properties similar to those of identified P-cells. Therefore, they were classified as P-cells and were treated as such in the analysis.

Finally, we recorded from units located outside identified P-cell layers with discharge suggesting that they were mossy fiber afferents, including very low frequency or no spontaneous background discharge, initial positive-going spike waveform potentials, and recording locations adjacent to layers where identified P-cells were found. We classified units of this type as cerebellar input units.

All unit activity was amplified and filtered by conventional recording equipment and passed through a window spike discriminator. Both the raw signal and the output of the window detector were displayed on an oscilloscope and piped through a speaker for auditory monitoring of cell and discriminated activity. The discriminated data were then output to a PDP-11 computer and stored on disk for later analysis.

Lesions

Lesions were made by first recording the activity of cerebellar neurons in previously mapped regions of the uvula. The recording electrode was then replaced by a 30-gauge stainless steel cannula that was advanced through the same guide tube that had just been used to direct the microelectrode for the unit recording. The guide tube was left in place during the replacement of the microelectrode by the injecting cannula. Great care was taken to place the cannula tip at the same depth as uvular units that had just been recorded.

We first injected 10–15 μl of 2% or 4% lidocaine with an infusion rate of 1 μl/min at each site in an attempt to make reversible lesions. We began recording eye movements immediately after the 10–15 min injection period of lidocaine, but found that the effects of lidocaine began to diminish within 20 min after we began to record eye movements. Therefore, we had to make repeated injections (up to a maximum of four) of this drug at each site to be able to complete our eye movement measurements. With these injec-

tion amounts we found that the effects of the lidocaine were not fully reversible, suggesting that mechanical trauma around the injection site may have contributed to creating the lesion. If more than one site were explored on a given day, we were careful to make sure that the cannula was displaced by at least 2 mm.

We followed the lidocaine injections with an ibotenic acid injection at one site in each animal (or two sites in one animal) where a large effect of the lidocaine on eye movements had been produced. The latter injection was 2–4 µl of ibotenic acid (20 µg/µl in 0.1 M phosphate buffer), perfused at a rate of 0.2 µl/min. The injecting cannula was left in place for ~15 min and then was slowly withdrawn. All eye movement measurements of the effect of ibotenic acid were begun on the day following the injection.

Location of recording sites and lesions

Microelectrode tracks were made in parasagittal planes located from 0.5 mm from the midline and extending 3 mm lateral on each side. The 1-mm wide longitudinal strip on the midline was not targeted for recording, to avoid hitting the sagittal sinus. The placement of the guide tube tip in cerebellar tissue below the tentorium minimized the possibility of deviation of the microelectrodes away from a targeted position in the parasagittal plane.

Before the animals were killed, several electrolytic marker lesions were made at selected sites in the uvula which were not also injection sites by passing d.c. at 20 µA for 20 s through the tip of a tungsten microelectrode. Histological material was obtained by deeply anesthetizing the animal with pentobarbital and perfusing with buffered 10% formalin. Frozen serial sections (60 µm thick) of the uvula were cut in the parasagittal plane, and every other section was subsequently stained with cresyl violet. Electrode tracks were reconstructed from the locations of the recovered marker lesion sites, and an attempt was also made to further reconstruct alternating P-cell and fiber layers from notes taken on each track concerning activity at these points.

Paradigms

Monkeys were initially trained to fixate and to track a moving light spot (0.25° in diameter) generated by an oscilloscope projector (spot luminance 2 cd/m^2). The spot was backprojected onto a 90×90° tangent screen located 50 cm in front of the animal. Liquid reward was given when the animal kept its eye within a small, software-controlled window (usually±2°) surrounding the position of the target. Eye position was determined with the magnetic-field search-coil method, which had a resolution of 0.25° and a bandwidth of 1 kHz. Smooth-pursuit data were sampled at 500 Hz and OKN data at 100 Hz and then stored on disk for off-line analysis.

To elicit smooth pursuit, a laboratory microcomputer generated signals to move the spot smoothly using the jump-ramp paradigm (Rashbass 1961). The speed and direction of the spot were randomly selected from the set of 10, 20, or 40°/s in four directions along horizontal and vertical axes. Visually guided saccades were generated by stepping the same target in these directions to eccentric positions at 5, 10, and 20°. These were the standard parameters we used, but they were adjusted when the neuron was more sensitive within a different range.

Optokinetic stimulation was provided by rotating a drum about its vertical axis at constant speeds of either 20, 40, or 100°/s. The drum was marked on the inside with alternating light and dark stripes, each with random widths between 1 and 8° of visual angle. The stripes were illuminated at a mean luminance of 9.1 cd/m^2 (contrast 0.82). In a typical trial, the drum was accelerated to the specified speed with the drum lights off. The drum lights were then turned on, presenting the animal with a step-like increase in visual surround velocity. Drum rotation continued at a constant velocity for about 30 s, after which time the drum motor and lights were turned off, placing the animal in total darkness. Some cells were tested when the drum lights were reilluminated for 3–6 s (with the drum now stationary) following the offset of optokinetic stimulation and the onset of OKAN, to see how they responded during a period of visual "dumping," which immediately reduces the velocity of the OKAN. Some neurons were also tested during suppression of optokinetic nystagmus. For suppression paradigms, the monkey fixated a small, stationary light-emitting diode (LED) located inside the drum during illuminated rotation epochs.

The animals were also subjected to pure vestibular stimulation by rotating their heads and bodies en bloc in total darkness. The whole-body vestibular stimulation was done with a velocity servo-controlled turntable that rotated about a vertical axis. Angular velocity of the turntable, and hence the animal's head, was monitored by a tachometer that was attached directly to the platform drive shaft. Room lights were illuminated between trials to prevent dark adaptation of the animals.

Data analysis

Eye movement and spike data were analyzed initially on a PDP 11/73 and more recently on a PC/AT compatible computer. Eye position signals were differentiated by analog hardware to produce eye velocity signals, and saccades were removed from velocity records by manual selection and/or a saccade-detection algorithm based on an acceleration criterion. Neuronal data were first converted to a spike density function (a convolution of raw spike train data from each trial with a Gaussian time function), which provides a continuous representation of spike firing probability (Richmond et al. 1987). The width (σ) of the Gaussian standard used was 10 ms for pursuit and 100 ms for OKN. We started out using a computer program to fit cells with an exponential function, using a nonlinear curve-fitting routine, provided by Matlab (The Mathworks) to determine the time constant of change for a single neuron. However, it proved to be more expedient to determine graphically the amount of time that it took the response to rise or fall to 67% of its final rate, and since the two methods where in close agreement for the cells that were tested with both methods (graphic: latency 3.0, τ=2.4; computer: latency 3.9, τ=2.5; n=12), we used the graphic method for our analysis. Eye movement records were fit by computer using a Matlab routine.

To quantify the directional specificity of units responding to drum rotation, a directional index (DI) was computed (Baker et al. 1981) for each neuron, using the formula:

$$DI = 1 - \frac{DNP}{DP} \quad (1)$$

where ΔP is the maximum observed change in firing rate from the spontaneous activity of the cell in the preferred direction of drum rotation, and ΔNP is the change for the nonpreferred direction. Using this formula, a neuron with DI=0.8 would be modulated 5 times stronger in the preferred than in the nonpreferred direction. Since uvula neurons could be excited or inhibited by optokinetic stimulation, we defined the direction of drum motion associated with the largest absolute value of change as the preferred direction. Excitatory and inhibitory modulations were treated as positive and negative respectively; therefore, a cell had maximum directional selectivity if DI=2.

Results

Single units

Population sampled

We recorded 92 single cells in the uvulae of the three monkeys. From this sample, 78 were classified as P-cells and 14 were classified as uvular input units by the criteria described in Materials and methods. The activity of

58 of the total group of 78 P-cells was modulated most robustly by prolonged optokinetic drum rotation. An additional 8 P-cells were modulated only during the other tasks (pursuit or saccades) and 12 were not modulated by any of the stimuli or behavioral tasks that we used in these experiments. In contrast, the uvular input units predominately responded during pursuit, saccades or short duration (about 2 s long) textured background motion that was projected on the tangent screen in front of the animals. These units were presumed to be mossy fibers originating from pontine gray areas or the vestibular nuclei, brainstem areas which provide the majority of input to the uvula (see Keller and Heinen 1991 for a review). Reconstruction of the recording sites of the 66 P-cells that were activated during our visual or oculomotor paradigms showed that units were recorded throughout the uvula, although the recording sites were concentrated in the dorsal uvula (folia a and b). The reconstructions indicated that most (56/66) of the units were located at least 0.5 mm lateral to the midline, placing them at the boundary between sagittal zone A and B or in zone B (Voogd and Bigaré 1980). The other 10 cells were located within the central 1-mm of the uvula (zone A), possibly because the penetrations were tilted slightly or the vermis was not centered in the recording chamber. We could not determine a functional difference between the types of P-cells with respect to either dorsoventral (folia) or mediolateral (longitudinal zone) location of the recording sites.

Purkinje cell responses during optokinetic eye movements

All P-cells recorded in the uvula had a spontaneous background discharge as the monkeys rested quietly in the dark experimental room (mean rate 55 spikes/s, range 19–111; n=58). Response modulations from the spontaneous level of activity were produced by constant-velocity optokinetic drum rotation and the ensuing ocular OKN. The most typical type of response is illustrated in Fig. 1 by two uvular P-cells. The modulation could be described qualitatively as a direction-dependent increase or decrease in discharge rate from the spontaneous level of activity. Interestingly, the activity of most uvular neurons was not modulated immediately after the onset of the optokinetic stimulation (as would be expected if the response were reflecting a strict visual or eye movement influence), but usually occurred instead only after several seconds of stimulation when OKN was well underway. Most of the cells were directionally selective, and their activity level was usually sustained throughout the period of drum rotation or only partially sustained (Fig. 1). We fit the initial response (excitation or suppression) for the direction of OK stimulation that produced the largest magnitude of response with a single-exponential time constant (see Materials and methods). An example of the fit obtained for the upper cell of Fig. 1 is shown in the upper inset.

When we attempted to fit a single-exponential to the response profiles of the buildup in OKN slow-phase eye

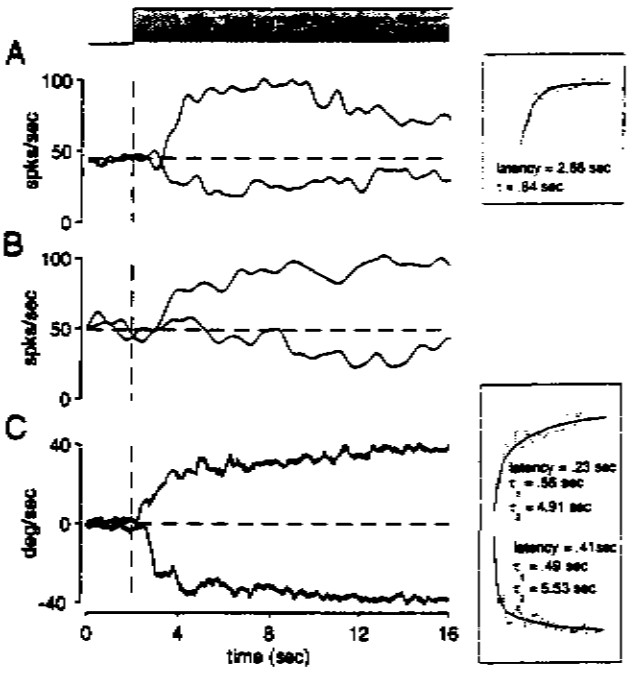

Fig. 1A–C Modulation of typical Purkinje cells (P-cells) recorded in the uvula of monkey BA during optokinetic (OK) nystagmus. **A, B** Spike density records for discharge of two P-cells. Averaged neural discharge during rightward drum rotation shown as *up* for each unit and *down* during leftward rotation. Three trials in each direction were averaged to obtain each response. **C** Stereotypical mean OK eye velocity responses in monkey BA (after removal of saccades). Again, rightward eye movements are shown as *up* and leftward *down*. The *insets on the right* illustrate examples of the fitting technique used to compute unit response latency and time constant (*upper box*) and optokinetic eye movement latency and time constants (*lower box*). (See text for details of the fiting technique.) Illuminated drum state is shown at the *top*. Drum speed was always 40°/s. *Dashed vertical line* indicates drum onset. The baseline cell rate and eye movements are shown by *dashed horizontal lines*

movements (lowest pair of traces), the optimization routine failed to converge or gave poor approximations, probably due to the two-phase nature of the primate OKN response (Cohen et al. 1977). However, two exponentials gave a better fit (lower insets in Fig. 1). OKN in all three monkeys was very stereotyped over recording sessions. We averaged the parameters obtained from fits of OKN in our animals over three daily sessions to allow us to compare the buildup in eye velocity with the time-course of modulation of our cells. The analysis for OKN eye movements yielded a mean latency of 275 ms, and two time constants: τ_1=0.51 s and τ_2=5.53 s, respectively.

The distributions of response latencies and time constants for 52 of the 58 optokinetic-responsive P-cells for which we had sufficient data to quantify these parameters are given in Fig. 2. This population of cells responded with a mean latency of 3.5 s (SD 2.6) following the onset of optokinetic stimulation and a mean time constant of 1.8 s (SD 1.2).

It is clear from the data shown in Fig. 2 that the responses of uvular P-cells to optokinetic stimulation, while grossly similar to OKN, were not quantitatively re-

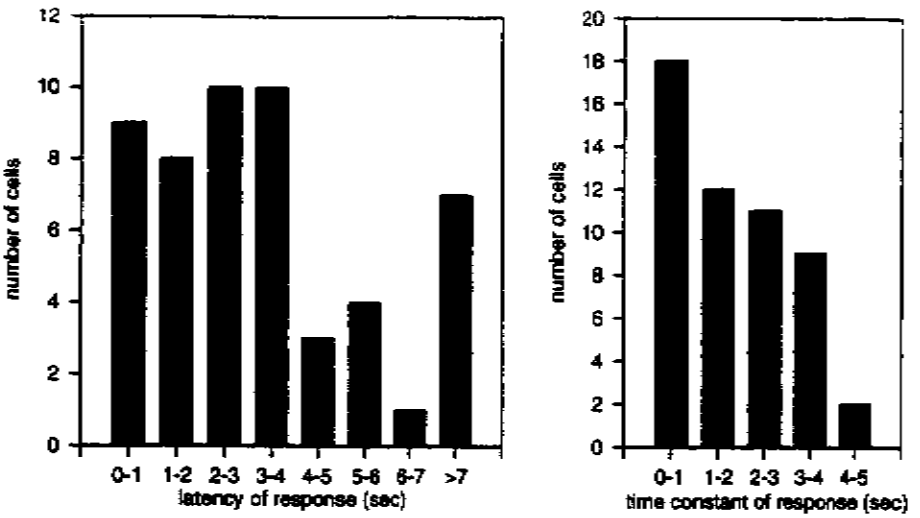

Fig. 2 Summary of latencies and time constants for 52 P-cells with response properties similar to the cells illustrated in Fig. 1. Data on the *left* show distribution of latencies for unit responses relative to drum onset. Data on the *right* show distribution of the single time-constant fits for unit responses for the direction of optokinetic stimulation that produced the largest absolute response (excitation or suppression)

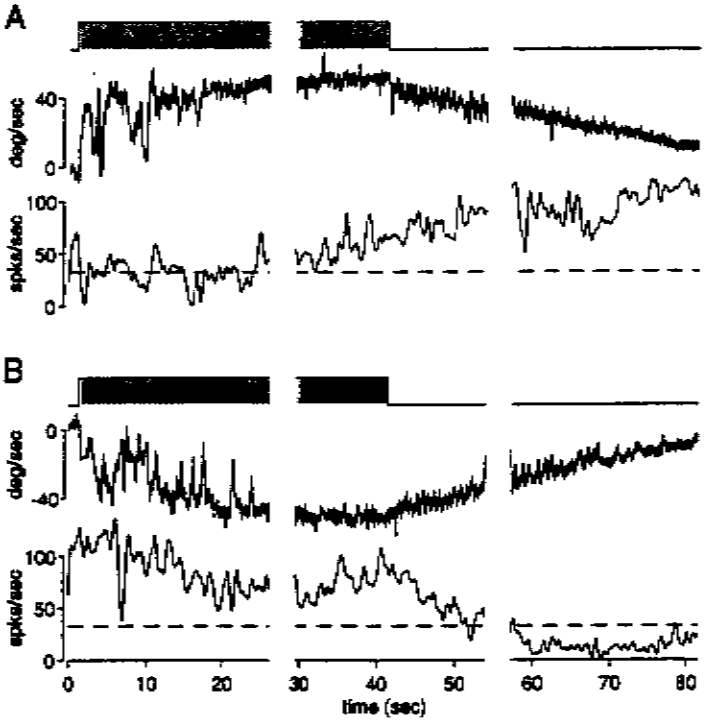

Fig. 3A, B Modulation of a longer-latency optokinetic P-cell during and following drum rotation. **A** Drum rotation at 40°/s right for 40 s. After a long latent period following the onset of drum rotation, unit activity increases very slowly and continued to build even after drum was stopped and optokinetic afternystagmus (OKAN) decayed. **B** After about 5 s beyond the end of the data acquisition shown in A, drum direction was reversed (now leftward). Note that the activity of this neuron slowly decreased after reversal of the direction of optokinetic stimulation, and continued to decrease during OKAN, eventually being suppressed below its original spontaneous level. The breaks are approximately 3-s periods of time, when stored data was written to the computer's disk. Other details the same as in Fig. 1

lated to either of the two standard phases used to describe the eye movements. Specifically, the unit responses do not begin until after the initial phase of OKN is over and saturate early as OKN continues its slow, second phase of gradual buildup. Despite the fact that uvula neurons responded robustly during drum rotation, we found the lack of exact temporal correspondence with the eye movement puzzling. To ensure that the response was in fact related to the motion processing or the eye movement, and not some general function such as arousal, we assessed the extent that the cell activity corresponded with the direction of drum rotation by computing a DI (see Materials and methods). Fifty-eight percent of the 52 P-cells we tested were strongly directional, having a DI of 0.8 or greater; 14% were moderately directional, with a DI between 0.4 and 0.8, and 28% showed little or no directionality, with a DI below 0.4.

The responses recorded in this group of P-cells when optokinetic stimulation was stopped by turning the rotating drum lights off were extremely variable, making it difficult to quantify the drum-off response. Many of these cells still had not begun to return to their spontaneous level until after the OKAN had stopped, beyond our data sampling epoch. The mean time constant of the transition back to spontaneous levels for the cells that did return to their baseline firing rate within the period of data collection (n=38) was 2.0 s. Again, the time constant did not correlate well with the eye movements, which decayed with a mean time constant during OKAN of 15.0 s.

Six of the P-cells in our sample responded with considerably longer latencies than the type of cell shown in Fig. 1. The response of these cells was modulated at a more gradual rate, sometimes not even reaching a steady

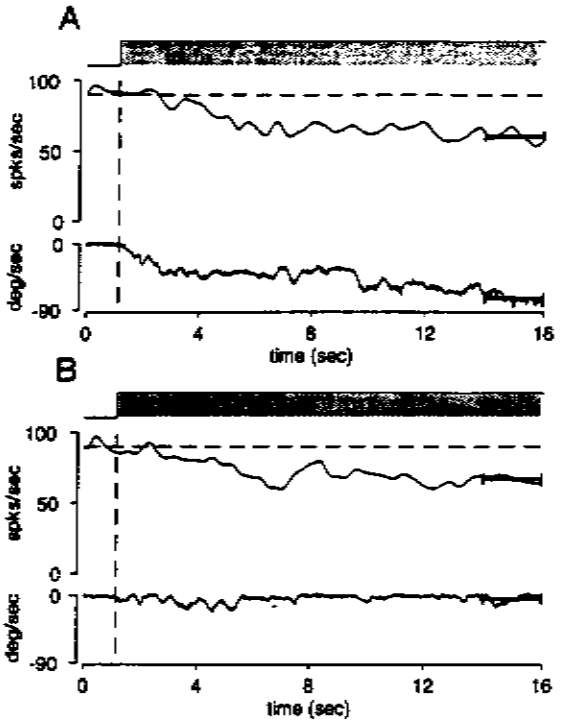

Fig. 4A, B The effect of optokinetic eye movement suppression on the response of a typical optokinetic uvular P-cell. **A** Cell discharge and slow-phase eye velocity during drum rotation with no fixation point (normal condition). **B** Activity of the same neuron and slow-phase eye velocity when the monkey attempts to fixate a small stationary spot to suppress optokinetic nystagmus. Drum velocity 100°/s left in both sets of trials. The *horizontal bars at the right* superimposed on the unit response and eye velocity traces represent the period of time over which each was averaged to produce the response metric (see text for details). Two trials were averaged to obtain each record. Other details as in Fig. 1

level during the 30-s period of optokinetic stimulation (Fig. 3A). The cell shown here had a response latency of about 25 s, and its discharge rate continued to increase after optokinetic stimulation ended and throughout the period of OKAN. The cell maintained the elevated level of discharge for several seconds after the direction of drum rotation was reversed. Optokinetic stimulation in the opposite direction slowly drove the discharge back to and below its original spontaneous rate. Technical limitations prohibited us from determining how much time these units required to reach a steady state response. Nevertheless, it is clear that such responses, although related to the optokinetic stimulation because of the directionality, could not directly regulate OKN or OKAN given their sluggish response dynamics.

Speed selectivity

We tested most cells with two drum speeds, 40°s and 100°/s. None of the parameters of the neuronal response, i.e., latency, time constant, or peak discharge, varied in a consistent fashion as speed was changed. Several cells were also tested with a 20°/s drum speed to determine whether they were more sensitive to velocities in a lower range. These P-cells showed virtually identical responses to the 20°/s drum rotations as to the other speeds.

OKN suppression

We tested 11 of the 58 P-cells that responded to optokinetic stimuli while the monkey actively suppressed OKN by fixating a stationary visual target during drum rotation (OKN suppression). OKN suppression markedly decreased OKN slow-phase eye velocity, and our monkeys were often able to completely abolish the nystagmus for extended periods. However, cells still responded as they did during normal OKN (Fig. 4).

This observation was quantified by measuring mean unit response (from the cell's spontaneous level) over a 2-s epoch that began 14 s after the drum started to move in the preferred direction both during normal OKN and suppression. The ratio of the response during suppression to the response during OKN was computed for each of the 11 units, yielding a mean value of 0.88 (±0.23 SD). A similar ratio of mean slow-phase eye velocity during suppression to that during OKN was computed, but yielded a very different mean value of 0.11 (±0.09 SD). The much greater suppression of eye movements suggests that the visual motion created by the rotating drum, and not the eye movements per se, was the primary cause of P-cell activation.

Saccadic response

A few cells (n=6) exhibited the typical overall response pattern to drum rotation (see Fig. 1), but superimposed on the sluggish response were short bursts of activity that were time locked to each quick-phase eye movement (saccades). The duration of the bursts was similar to duration of the saccades and preceded saccade onset by an average of only 3.6 ms. They were usually stronger for saccades in one direction, and were still present for saccades that occurred during OKAN in the dark. Therefore, the quick-phase responses were not produced by retinal stimulation during saccades.

Responses during rapid visual suppression of OKAN

Sixteen neurons that were kept isolated for long enough were tested with a brief period (3 s or 6 s) of stationary, full-field visual stimulation during OKAN (see Materials and methods). Such stimulation significantly reduces the length of OKAN and has been referred to as a "visual dump" (Cohen et al. 1977). Only 6 of the 16 tested P-cells were affected by visual dumping. The most robust response that we recorded is illustrated by the P-cell shown in Fig. 5. The activity of this cell was modulated above its spontaneous rate by optokinetic stimulation to the right. The activity of the cell was rapidly suppressed

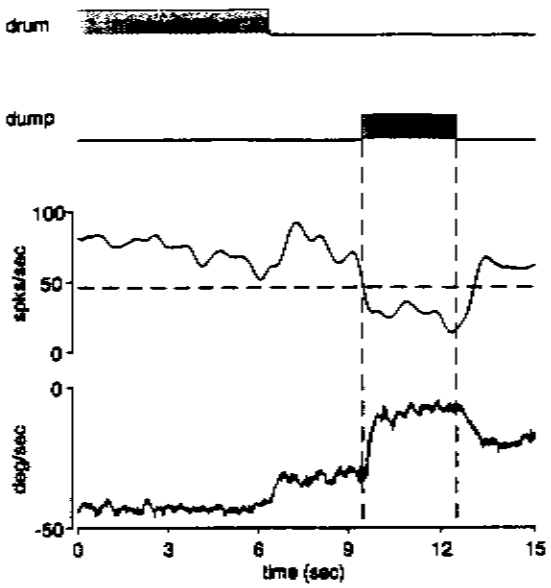

Fig. 5 The effect of a "visual dump" on the discharge of a uvular P-cell during OKAN. The lights were illuminated inside the stationary drum during the epoch indicated by the *vertical dashed lines*. *Upper two traces* show illuminated drum rotation and dump states. The *middle trace* is the activity of the cell (mean of three trials) aligned on dump onset. The *dashed horizontal line* indicates the spontaneous activity of the cell. The *bottom trace* shows mean slow phase eye velocity during drum rotation, during ensuing OKAN in the dark and during the period of the visual dump

to below its spontaneous level following the onset of drum reillumination. After the drum lights were again extinguished the cell returned rapidly to the elevated rate that was present prior to the dump. The other cells responded in a similar, although less robust, fashion during the dumping period.

Responses during vestibular stimulation

Thirteen P-cells that responded to optokinetic stimulation were tested for vestibular responses with constant-velocity angular head rotation in the dark. Six of the cells tested responded to the vestibular stimulation. Interestingly, the responses were very similar to those occurring during optokinetic stimulation. Specifically, the cell did not begin to respond until well after chair rotation commenced. Cell activity was then excited or inhibited for a period that could again exceed the period of stimulation. Therefore, as with drum rotation, chair rotation produced responses that somewhat resembled the eye movements, but which could not be linked directly to their temporal characteristics. Because of the small sample size, we did not attempt to further quantify vestibular responses.

Responses during pursuit eye movements

A small number (n=17) of uvular units responded when the monkey smoothly pursued a moving spot of light (pursuit units). Of the 17 units, 11 were classified as P-cells, and the remaining six were categorized as cerebellar input units (see Materials and methods). Typical responses of two units are shown in Fig. 6. Some cells responded after smooth eye tracking was initiated (Fig. 6A,B).

A unit with a relatively short response latency (less than 100 ms) can be seen in Fig. 6C. The response here began before the eye started to move. We recorded only eight units that responded before the eye movement. Such short response latencies probably reflected visual input to the uvula; however, since pursuit units were rarely encountered, we made no attempt to dissect the visual from the nonvisual or extraretinal components of the response. Pursuit units could also be excited or inhibited during pursuit, and most were directionally selective (mean DI=0.69).

Lesions

After the single-unit experiments were completed, chemical lesions were made in the uvula of each of the three monkeys (see Materials and methods). We made lidocaine injections at eight different sites in the three animals and effects on eye movements were obtained at six of the sites. The two sites where no effects were noted were located 2 mm away from sites where effects had been measured, suggesting that the effective spread of lidocaine was no more than 2 mm. A total of four ibotenic acid injections were made. We recovered three clear lesion sites in the histological material where ibotenic acid had been injected. These three lesion sites are shown in Fig. 7. In one animal (BA), in which repetitive lidocaine and two ibotenic acid injections were made at two sites 2 mm apart, a large lesion was found in the stalk of the uvular lobule and in a few of the surrounding folia. Because fibers in the white matter and P- and granular cells were destroyed at this site, we believe that this lesion was produced by a combination of mechanical disruption, due to the multiple lidocaine injections, and the neurotoxic effects of the two ibotenic acid injections. The lesion in BA extended out from the midline on the left side almost to the lateral border of the vermis (section at 3.0 L in BA) and, therefore, probably disrupted a large part of the input and output of the uvula on this side of the vermis. In a second animal (JE), the lesion was located approximately on the midline and primarily affected folia a of the dorsal uvula, but also a small portion of adjacent lobule VIII. The lesion destroyed mostly cell bodies, but again some surrounding fibers were damaged owing to mechanical effects. The lesion in JE was less than 1.25 mm in mediolateral extent. The lesion in the third animal (AN) destroyed a portion of folia a and b of the left uvula and was only ~1.0 mm in mediolateral extent. All three lesions produced some oculomotor abnormalities. However in all animals, even BA, the animal with the largest lesion, oculomotor behavior was vir-

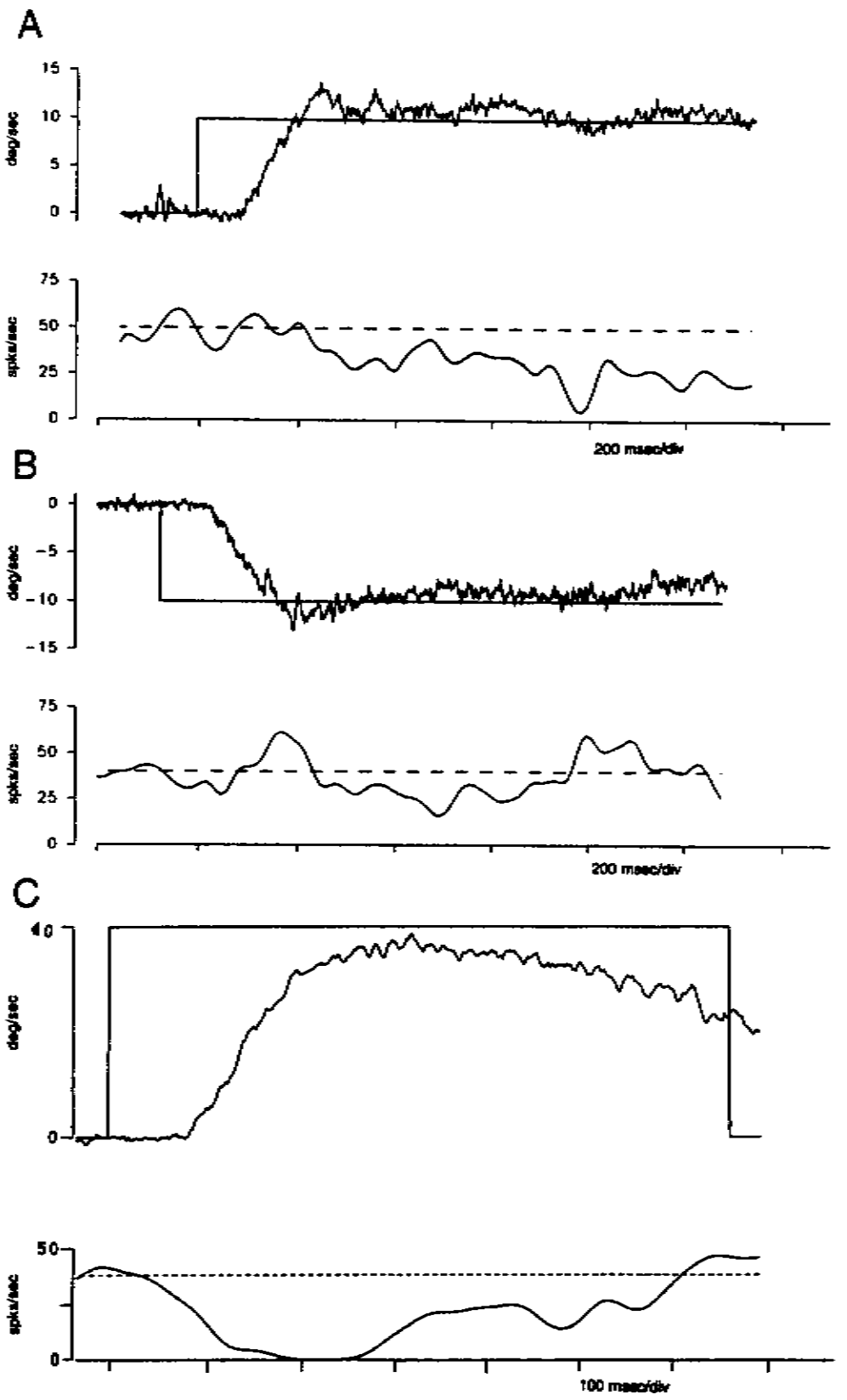

Fig. 6A–C Smooth-pursuit-related responses of uvular units. **A** Response of unit during tracking of a spot at 10°/s right, averaged over five trials. In this direction the unit showed a clear suppression of activity below spontaneous level (*horizontal dashed line*) beginning ~200 ms after the onset of target motion which continued throughout the trial. **B** During leftward pursuit, the activity of the unit fluctuated about the spontaneous level and was not clearly modulated. **C** Activity of another uvular unit during tracking at 40°/s to the right, averaged over five trials. Here, the response started before the eye movement began, possibly reflecting visual input to the uvula. Note the different time scale in **A** and **B** compared with **C**. All eye velocity records have been desaccaded. Velocity of the tracking spot shown by the *solid lines*

tually normal 2–3 days after the injection of ibotenic acid.

Because most uvular cells responded during constant-velocity OK stimulation, we were surprised to find that our lesions had the greatest effect on smooth pursuit. Even more interesting was the nature of the pursuit deficit. Instead of the decrease in smooth eye velocity seen with most other cerebellar lesions (Zee 1982; Keller 1988) eye acceleration *increased* during pursuit initiation (open-loop gain) for pursuit generated contraversive to

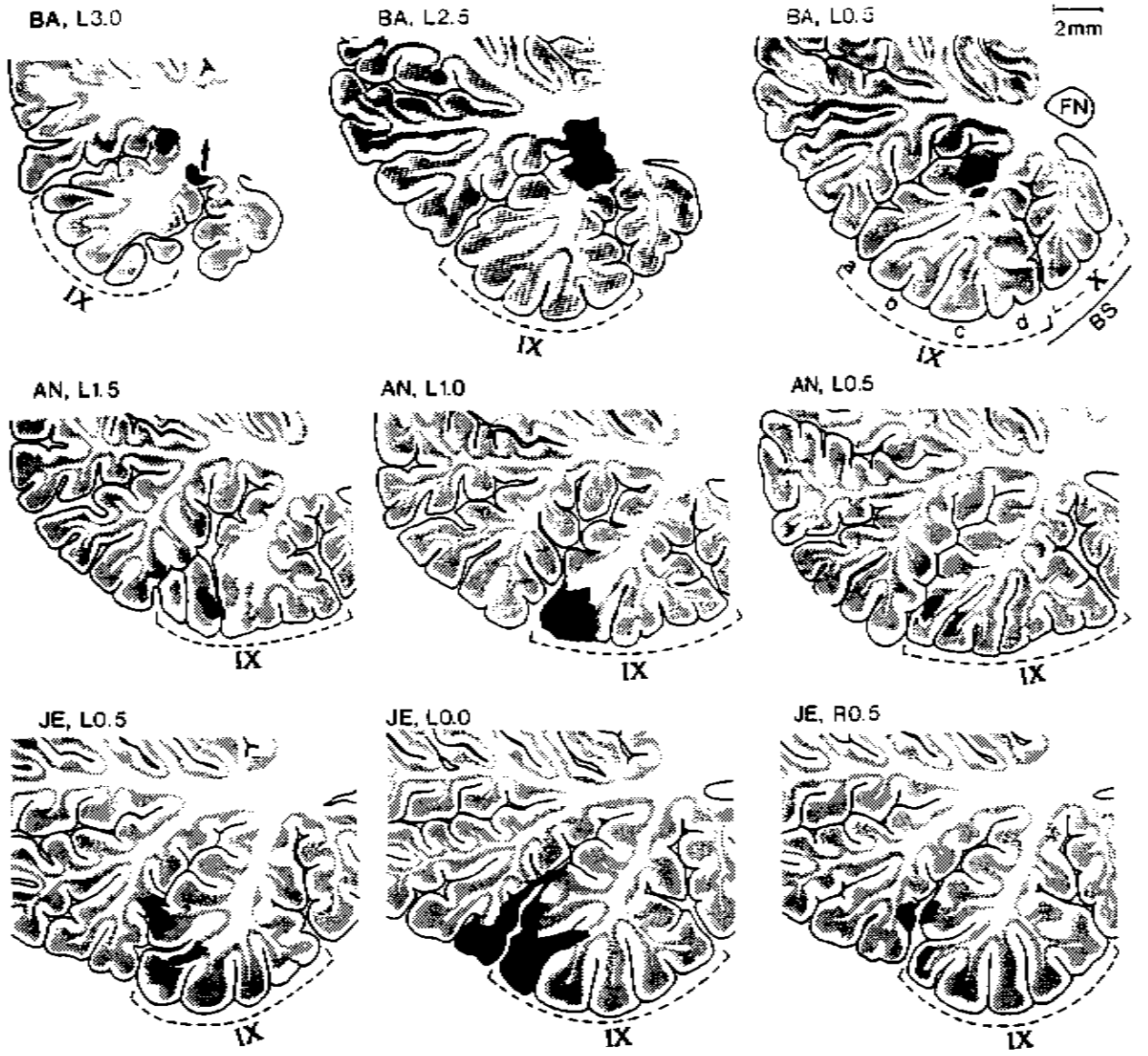

Fig. 7 Schematic showing the extent of the lesions in the three animals. Each *row* shows the results for one animal (BA, AN, or JE). The *middle section in each row* shows a sagittal section near the center of the largest extent of the lesion for that animal. The *flanking sections* are close to the lateral borders of each lesion. In *all sections* the distance of the section from the midline is given in millimeters for left (*L*) and (*R*). The uvula (lobule *IX*) and the nodulus (lobule *X*) are marked with *dashed brackets* and the folia of the uvula are indicated with *a,b,c,* and *d*. For clarity in all other sections only the uvula is marked by a *dashed bracket*. *Calibration at top right* applies to all sections. Sections are oriented so that stereotaxic vertical is *up*. The rostral edge of each section is on the *right*. Lesions are indicated in all sections by *solid shading*. (*FN* fastigial nucleus, *BS* brainstem)

the lesion site (Fig. 8). The largest effect, caused by a major disruption of function of the left uvula in BA can be seen in Fig. 8A.

During pursuit of 20°/s ramp target motion, BA had a peak mean eye velocity during the first 100 ms after contraversive pursuit began that reached 36.1°/s (SE 3.2°/s), in contrast to 16.4°/s (SE 0.9°/s) before the lesion. However, by ~600 ms after pursuit initiation, maintained eye velocity had almost returned to normal, suggesting that only the initial (open-loop) phase of the pursuit response was affected by the lesion. Pursuit of ipsiversive target motion was virtually unaffected. Pursuit eye movements of the other animal with a smaller unilateral lesion (AN) was similarly affected, but to a lesser degree than seen in BA. An interesting result was seen following the midline lesions in JE. This animal showed a greater open-loop response for *both* directions of pursuit (Fig. 8B). A ratio of initial eye acceleration (averaged over the first 100 ms of pursuit) in the lesioned animals to that seen before the lesions was computed, and the results are summarized in Fig. 9. The same qualitative effect on smooth pursuit eye movements was measured on the day after ibotenic acid injection, but almost complete recovery was obtained by the 3rd day after ibotenic acid injection.

The effect of uvular lesions on OKN was less impressive than the effect on pursuit, despite the fact that P-

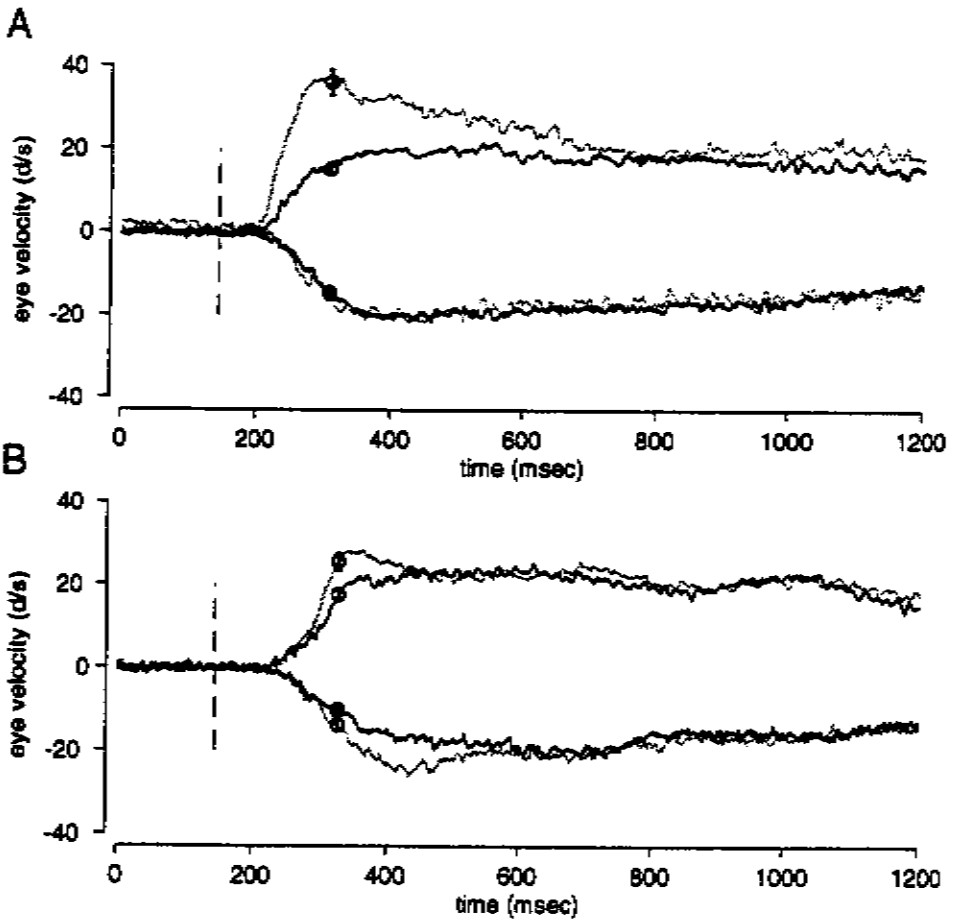

Fig. 8A, B Effect of uvular lesions on smooth-pursuit eye movements. **A** Averaged eye velocity traces before (*dark curves*) and after (*lighter curves*) the lesion in BA, the animal with the large left uvular lesion. *Top* is rightward pursuit, *bottom* leftward. Target speed was 20°/s. Note the much greater initial eye velocity for contraversive pursuit after the lesion, but that ipsiversive pursuit was virtually unaffected. **B** Eye velocity traces in the animal with a bilateral uvular lesion (JE). This animal showed higher initial eye velocity for both directions of pursuit. Eye movement recording started 10 min after an injection of lidocaine was completed in both **A** and **B**. The effect remained in BA when testing was done 1 day following the ibotenic acid injection. All traces have been desaccaded and aligned on the start of target motion (*vertical dashed lines*). *Small open circles* indicates the mean eye velocity 100 ms after pursuit initiation, with *bars* showing SEM. Note SE is often smaller than the symbol. Five individual trials were averaged to obtain each response

cells responded more clearly during optokinetic stimulation. For BA, contraversive drum rotation resulted in a larger initial optokinetic response, but the more slowly developing second (charging) phase of OKN was nearly normal (Fig. 10). We determined the mean initial acceleration over the first 200 ms of the optokinetic response. The first peak in optokinetic eye velocity normally occurred near this time in most animals. Note that BA had a very asymmetrical initial optokinetic response before the lesion, a feature that was not seen in the other two animals. For consistency, we measured the mean initial eye acceleration to the left during the same time epoch.

Leftward drum rotation yielded a slight decrease in the initial eye velocity for ipsiversive OKN and decreased steady-state eye velocity throughout the entire period of optokinetic stimulation, although BA showed the largest steady-state effect of any of the animals. Episodes of total loss of optokinetic slow-phase eye velocity even in the face of the constant-velocity, ipsiversive optokinetic stimulation, similar to that seen at the epoch marked by the asterisk in Fig. 10A, were commonly ob-

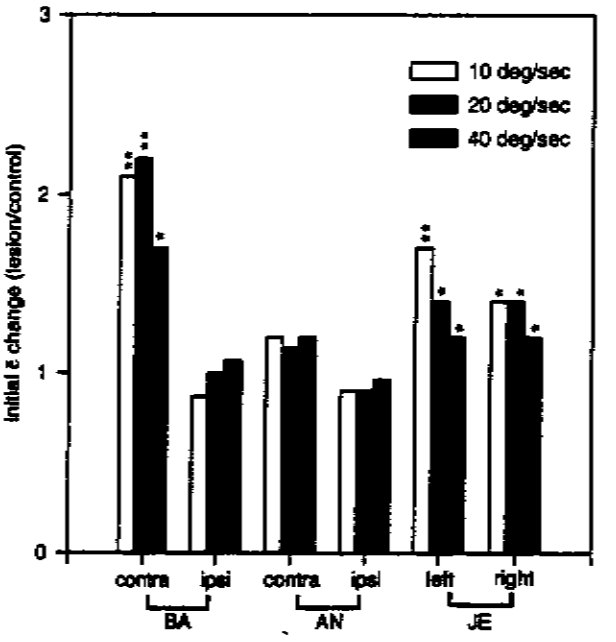

Fig. 9 Summary of smooth pursuit deficits in all three animal for three different target speeds and directions ipsiversive (*ipsi*) or contraversive (*contra*) to the lesion. The ratio of the mean initial eye acceleration over the first 100 ms of the pursuit response after the lesion to a similar measure before the lesion is shown for each animal for each direction and speed. Animal J.E. had an approximately bilaterally symmetric lesion, therefore labels are *left* and *right*. Eye movement recording in all cases was begun 10 min after lidocaine injection. Significant initial eye acceleration differences before and after the lesion are indicated by *asterisks* (*t*-test: ** $P<0.001$, * $P<0.05$). At least three trials and usually five trials were averaged to obtain these results

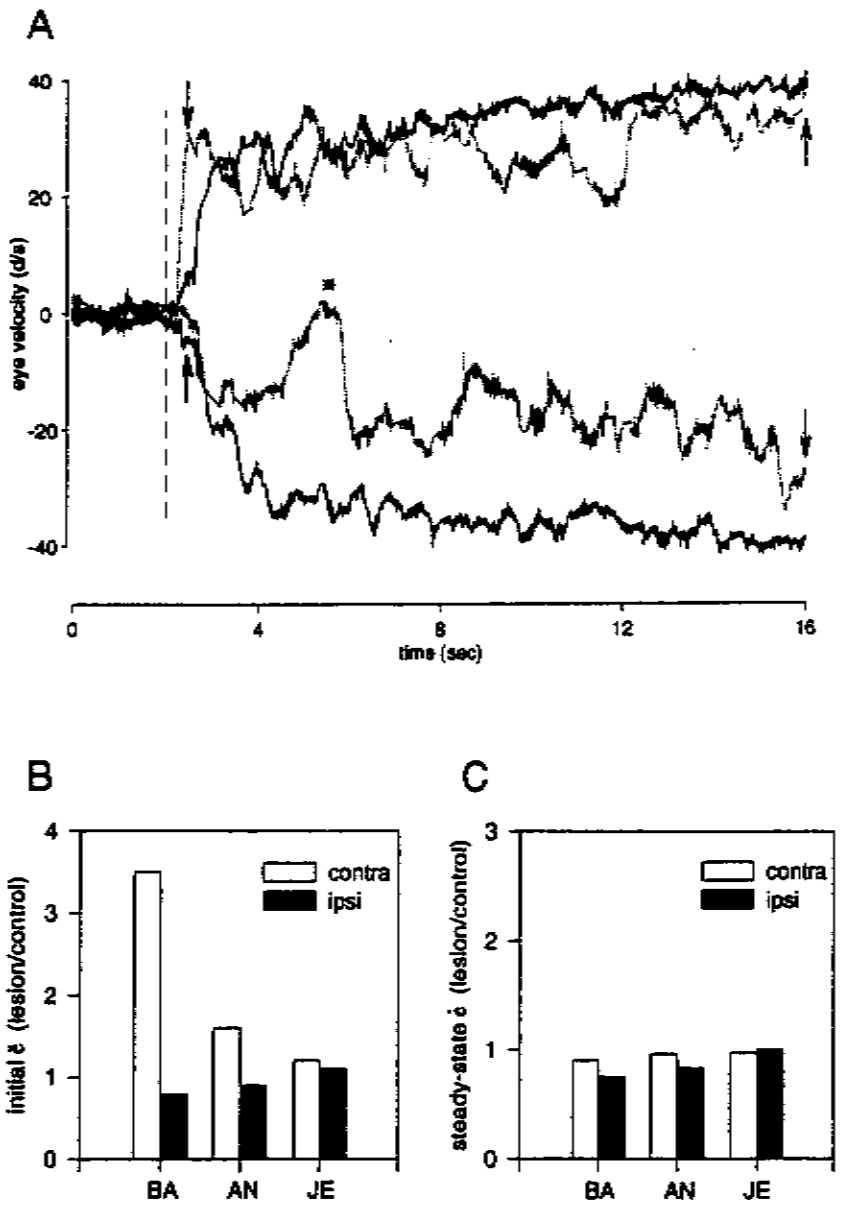

Fig. 10A–C Effects of uvular lesions on OKN. A Mean slow-phase eye velocities in animal BA before (*dark curves*) and after (*lighter curves*) a lesion of the left uvula. Drum motion was 40°/s in each case, right (contraversive to the lesion) is shown *up* and left is *down*. Eye velocity is aligned on the onset of optokinetic stimulation (*vertical dashed line*). Three trials are averaged for each condition. The *pair of vertically aligned arrows on the left* indicates the point in time that the mean initial eye acceleration was computed for each condition. The *pair of arrows on the far right* indicates the time that "steady-state," slow-phase eye velocity was computed (averaged over 100 ms). The *asterisk* indicates an episode when slow-phase eye velocity dropped to zero. **B** Summary of the effects of lesions on initial eye acceleration for both directions of OK nystagmus and for all three animals. **C** Summary of the effects of the lesions on steady-state eye velocity for both directions of optokinetic stimulation and for all three animals. Eye movement recording in all cases was begun 10 min after lidocaine injection

served. Both animals with unilateral lesions (BA and AN) showed a similar pattern of OKN deficits; however, the effect of the lesion on JE was minimal. A ratio of initial eye acceleration during OKN in the lesioned animals to that seen before the lesions was computed, and the results are summarized in Fig. 10B. We also determined the ratio of eye velocity 14 s into OKN to quantify the steady-state deficit (Fig. 10C). OKAN appeared to be normal in all three animals.

Figure 11 shows records from BA in trials where the lights were reilluminated briefly inside the stationary drum during OKAN following rightward (contraversive) optokinetic stimulation (visual dump). As mentioned before, dumping normally lowers OKAN slow-phase eye velocity substantially. This function did not seem to be affected by our lesions. No change in dump effectiveness was seen ipsiversively either, except that OKAN slow-phase eye velocity started with a lower value, since ipsiversive steady-state OKN was already reduced (see Fig. 10A above). Overall we have the impression that uvular lesions did not, or only minimally affected, the visual dumping of OKAN.

Discussion

Single-unit and lesion studies were conducted to explore the involvement of the cerebellar uvula in smooth-pursuit and visual-motion processing. The uvula receives projections from pursuit and visual regions of the pontine nuclei that are similar in density to those terminating in the cerebellar middle vermis and flocculus/paraflocculus (Brodal 1982; Glickstein et al. 1994). Does the neuronal processing done in the uvula complement that done in the middle vermis and flocculus for smooth-pursuit generation? We were surprised to find a very different

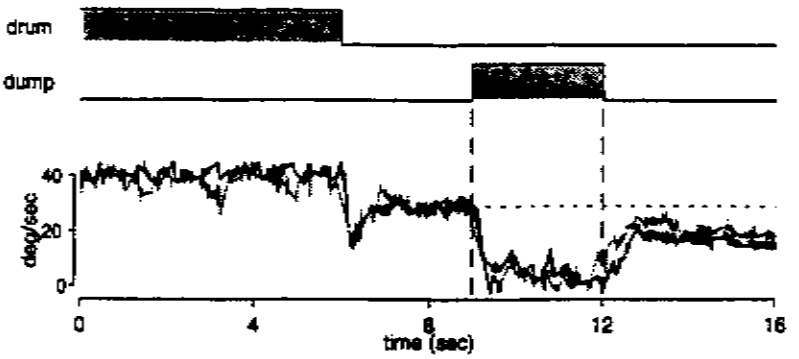

Fig. 11 Visual dump of OKAN remains intact after uvular lesions. Mean responses for two trials before (*dark curves*) and two trials after (*lighter curves*) the uvular lesion in BA *Upper two traces* as in Fig. 5. Records begin on the left near the end of a 30-s period of 40°/s rightward optokinetic stimulation. The drum then stops and the animal begins OKAN in the dark. The lights were illuminated inside the stationary drum during the epoch indicated by the *vertical dashed lines*. Eye movement recording in all cases was begun 10 min after lidocaine injection. The effect remained when testing was done 1 day following the ibotenic acid injection

type of signal present on the majority of uvular P-cells, as compared to that reported for similar visual stimulation in the latter areas. Although a few uvular neurons responded during smooth pursuit (see Fig. 6), the majority were better modulated by longer-term optokinetic stimulation. The optokinetic modulation had a long latency compared with previously reported pursuit or optokinetic responses in the flocculus or the middle vermis (Lisberger and Fuchs 1978; Miles et al. 1980; Suzuki and Keller 1988b), typically on the order of 2–5 s, and was usually maintained beyond the time when surround motion stopped. It could be that other types of sustained motion such as optic flow, looming, or expanding fields might affect the response of uvular neurons, although our apparatus did not allow us to test these possibilities.

Paradoxically, lesions to the uvula had a more dramatic effect on pursuit and the initial phase of OKN than on steady-state OKN and OKAN. Of even more interest was that uvular lesions resulted in a contraversive *increase* in eye acceleration during pursuit initiation and the initial phase of OKN. Although this is consistent with increases in oculomotor gain seen during vestibular stimulation in the rabbit following uvular lesions (Nagao 1983), lesions to other pursuit-related cerebellar cortical areas produce a decrease in the gain of smooth-pursuit eye movements (Keller 1988; Zee et al. 1981). Fuchs et al. (1994) have reported an increased gain for ipsiversive pursuit following unilateral lesions of the fastigial nucleus, an effect that is consistent with the increased gain for contraversive pursuit found in the current study.

A possible resolution of this paradox comes about by assuming that the uvula is not in the anatomical pathway that directly controls pursuit, but instead exerts a modulatory influence on brainstem centers normally involved in slow gaze control in order to maintain the correct gain

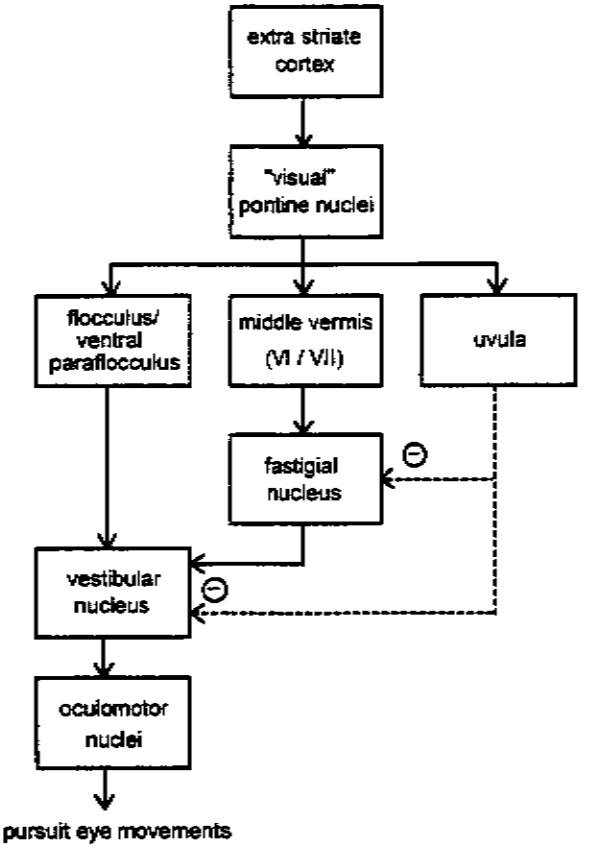

Fig. 12 Schematic of proposed functional connections of the uvula with the pathway involved in smooth-pursuit control. Visual motion processing occurs in extrastriate cortex, and the signal is gradually transformed into the command to move the eyes as it proceeds to the "visual" pontine nuclei and then through three parallel pathways in the cerebellar cortex. The two leftmost pathways (*solid lines*) constitute the traditional pathway that mediates pursuit and involve the flocculus/ventral paraflocculus and the midvermis. Output converges in the vestibular nucleus/prepositus hypoglossi complex and then goes to the oculomotor nuclei. The hypothesized pathway through the uvula (*dashed lines*) normally provides a tonic inhibitory influence on the vestibular nuclei either directly or through the fastigial nucleus. Sustained periods of abnormal motion change the output signal of the uvula, thereby adjusting the gain of smooth pursuit

in these pathways. Other cerebellar structures are known to participate in oculomotor gain control. Optican and Robinson (1980) concluded that the middle vermis served as an adaptive gain control mechanism for the saccadic pulse generator, since lesions there produce sac-

cades that overshoot visual targets (hypermetria). Similarly, the flocculus may participate in gain control of the VOR (Miles and Lisberger 1981). We hypothesize that the uvula modulates smooth pursuit through well-documented connections of the uvula with brainstem and cerebellar gaze centers (Fig. 12). The uvula projects directly to both the ipsilateral vestibular/prepositus hypoglossi complex and the caudal ipsilateral fastigial nucleus (Angaut and Brodal 1967). Projections from the caudal fastigial nucleus cross the midline and terminate in the contralateral vestibular nucleus (Batton et al. 1977; Noda et al. 1990). Thus, there are fairly direct pathways from each uvula to both vestibular nuclei. Since the lesions produced the strongest effect on contraversive eye movements, it appears that the uvula has stronger functional connections to the contralateral vestibular nucleus based on the assumption that at least a portion of the vestibular nucleus predominately generates ipsilaterally directed smooth movements (see Godaux et al. 1989 for a discussion of this assumption). This possibility is further supported by the fact that unilateral electrical microstimulation in the uvula evokes a nystagmus with a predominately ipsiversively directed slow phase (Heinen et al. 1992).

Because the typical P-cell response in our study roughly resembled that of a leaky integrator, it might be wrongly assumed that the uvula participates in velocity storage, since velocity storage, which is thought to be mediated by the medial vestibular nucleus/prepositus hypoglossi nuclei (Waespe and Henn 1977; Cannon and Robinson 1987), does not seem to be affected by uvular lesions. The velocity storage mechanism has been modeled as a leaky integrator that stores eye velocity during OKN and prolonged vestibular stimulation (Cohen et al. 1977), and the eye velocity seen during OKAN and following vestibular stimulation is the result of the decay of stored eye velocity in the integrator. In normal animals, the integrity of the storage mechanism is assessed by the resultant eye velocity relative to peak OKN velocity immediately after drum offset. Animals with uvular lesions show a similar amount of relative eye velocity after the drum is stopped (see Fig. 11), indicating that the velocity storage mechanism is intact. On close inspection, the pattern of discharge of P-cells that we recorded is also inconsistent with the uvula playing a role in velocity storage. Whereas the velocity storage integrator begins to charge almost immediately after the onset of OKN (Cohen et al. 1977), our uvular units did not respond until after a latent period that averaged 3.5 s after drum rotation began. Furthermore, the time constant of OKN eye velocity in monkeys is ~16 s (Cohen et al. 1977), but uvular P-cells reach full modulation with a mean time constant of 1.8 s.

We were surprised to find that our lesions had little effect on OKAN following a period of brief exposure to a lighted stationary surround (visual dump). In normal animals, the visual dump almost totally cancels OKAN (Cohen et al. 1977). Previous work has shown that combined lesions of the uvula and the nodulus result in a failure of the dumping mechanism, i.e., eye velocity is unaffected by the visual dump following the lesions (Waespe et al. 1985). We sometimes saw elevated eye velocity after the dump, but it seemed more related to the baseline drift of the eye than to a disruption of the dump mechanism. We attribute the difference in these findings to the fact that our lesions were restricted to the uvula, making it likely that dumping is mediated predominately by the nodulus. This finding remains paradoxical, since the uvula receives a much stronger visual pontine input than does the nodulus (Glickstein et al. 1994).

Our lesions, even in animal B.A. where most of the left uvula was functionally disrupted, produced primarily unilateral increases in pursuit gain that recovered in just 2–3 days. This is a short recovery time relative to that seen following lesions to other cerebellar areas. Animals still tracked poorly for up to 4 months following flocculus lesions (Zee et al. 1981). The gain of smooth pursuit after lesions of the middle vermis had only slightly recovered in 22 days (Keller 1988). These differences are probably related to the fact that our lesions were caused by punctate chemical injections that destroyed only a portion of the uvula, and in two cases were restricted to one hemisphere. In the other studies, either the flocculus (Zee et al. 1981) or the vermis (Keller 1988) was completely and bilaterally ablated by surgical procedures.

In conclusion, it appears that at least one function of the uvula is to regulate the gain of the smooth-pursuit system. It may do this by modulating its normally tonic inhibitory signal to the fastigial/vestibular nuclei when there are persistent and directionally biased periods of full-field visual motion. We believe that the uvula may be similar to other cerebellar structures, in that it can dynamically compensate for perturbations of a motor system and bring the system back into proper directional symmetry.

Acknowledgements This work was supported by National Institutes of Health Grant EY-06860, National Research Service Award 5 T 32 EY-97116-02, and The Smith-Kettlewell Eye Research Institute.

References

Angaut P, Brodal A (1967) The projection of the "vestibulocerebellum" onto the vestibular nuclei in the cat. Arch Ital Biol 105: 441–479

Baker JF, Petersen SE, Newsome WT, Allman JM (1981) Visual response properties of neurons in four extrastriate visual areas of the owl monkey (*Aotus trivirgatus*): a quantitative comparison of medial, dorsomedial, dorsolateral, and middle temporal areas. J Neurophysiol 45: 397–416

Batton RR, Jayaraman A, Ruggiero D, Carpenter MB (1977) Fastigial efferent projections in the monkey: an autoradiographic study. J Comp Neurol 174: 281–306

Brodal P (1979) The pontocerebellar projection in the rhesus monkey: an experimental study with retrograde axonal transport of horseradish peroxidase. Neuroscience 4: 193–208

Brodal P (1982) Further observations on the cerebellar projections from the pontine nuclei and the nucleus reticularis tegmenti pontis in the rhesus monkey. J Comp Neurol 204: 44–55

Brodal A, Brodal P (1985) Observations on the secondary vestibulocerebellar projections in the macaque monkey. Exp Brain Res 58: 62–74

Büttner U, Waespe W (1981) Vestibular nerve activity in the alert monkey during vestibular and optokinetic nystagmus. Exp Brain Res 41: 310–315

Büttner U, Waespe W (1984) Purkinje cell activity in the primate flocculus during optokinetic stimulation, smooth pursuit eye movements, and VOR-suppression. Exp Brain Res 55: 97–104

Cannon SC, Robinson DA (1987) Loss of the neural integrator of the oculomotor system from brain stem lesions in monkey. J Neurophysiol 57: 1383–1409

Cohen B, Matsuo V, Raphan T (1977) Quantitative analysis of the velocity characteristics of optokinetic nystagmus and optokinetic after nystagmus. J Physiol (Lond) 270: 321–344

Crandall WF, Keller EL (1985) Visual and oculomotor signals in nucleus reticularis tegmenti pontis in alert monkey. J Neurophysiol 54: 1326–1345

Fuchs AF, Robinson FR, Staube A (1994) Preliminary observations on the role of the caudal fastigial nucleus in the genration of smooth-pursuit eye movements. In: Fuchs AF, Brandt T, Büttner U, Zee DS (eds) Contemporary ocular motor and vestibular research: a tribute to David A. Robinson. Thieme, Stuttgart, pp 165–170

Glickstein M, Gerrits N, Kralj-Hans I, Mercier B, Stein J, Voogd J (1994) Visual pontocerebellar projections in the macaque. J Comp Neurol 349: 51–72

Godaux E, Cheron G, Gravis F (1989) Eye movement evoked by microstimulation in the brainstem of the alert cat. Exp Brain Res 77: 94–102

Heinen S, Keller E (1992) Cerebellar uvula involvement in visual motion processing and smooth pursuit control in monkey. Ann NY Acad Sci 656: 775–782

Heinen SJ, Oh KD, Keller EL (1992) Characteristics of nystagmus evoked by electrical stimulation of the uvular/nodular lobules of the cerebellum in monkey. J Vestib Res 2: 235–245

Kase M, Miller DC, Noda H (1980) Discharges of Purkinje cells and mossy fibers in the cerebellar vermis of the monkey during saccadic eye movements and fixation. J Physiol (Lond) 300: 539–555

Keller EL (1988) Cerebellar involvement in smooth pursuit eye movement generation: flocculus and vermis. In: Kennard C, Clifford Rose F (eds) Physiological aspects of clinical neuro-ophthalmology. Chapman and Hall, London, pp 341–355

Keller EL, Crandall WF (1983) Neuronal responses to optokinetic stimuli in pontine nuclei of behaving monkey. J Neurophysiol 49:169–187

Keller EL, Heinen SJ (1991) Generation of smooth-pursuit eye movements: neuronal mechanisms and pathways. Neurosci Res 11: 79–107

Langer T, Fuchs AF, Chubb MC, Scudder CA, Lisberger SG (1985) Floccular efferents in the Rhesus macaque as revealed by auto-radiography and horseradish peroxidase. J Comp Neurol 235: 26–37

Lisberger SG, Fuchs AF (1978) Role of primate flocculus during rapid behavioral modification of vestibuloocular reflex. I. Purkinje cell activity during visually guided horizontal smooth-pursuit eye movements and passive head rotation. J Neurophysiol 41: 733–763

McElligott JG, Keller EL (1982) Neuronal discharge in the posterior cerebellum: its relationship to saccadic eye movement generation. In: Lennerstrand G, Zee DS, Keller EL (eds) Functional basis of ocular motility disorders. Pergamon, Oxford, pp 453–461

Miles FA (1991) The cerebellum. In: Carpenter RHS (ed) Eye movements. (Vision and visual dysfunction, vol 8). Macmillan, London, pp 224–243

Miles FA, Fuller JH (1975) Visual tracking and the primate flocculus. Science 189: 1000–1002

Miles FA, Lisberger SG (1981) Plasticity in the vestibulo-ocular reflex: a new hypothesis. Annu Rev Neurosci 4: 273–299

Miles FA, Fuller JH, Braitman DJ, Dow BM (1980) Long-term adaptive changes in primate vestibulo-ocular reflex. III. Electro-physiological observations in flocculus of normal monkey. J Neurophysiol 43: 1437–1476

Mustari MJ, Fuchs AF, Wallman J (1988) Response properties of dorsolateral pontine units during smooth pursuit in the rhesus macaque. J Neurophysiol 60: 664–686

Nagao S (1983) Effects of vestibulocerebellar lesions upon dynamic characteristics and adaptation of vestibulo-ocular and optokinetic responses in pigmented rabbits. Exp Brain Res 53: 36–46

Noda H, Fujikado T (1987) Involvement of Purkinje cells in evoking saccadic eye movements by microstimulation of the posterior cerebellar vermis of monkeys. J Neurophysiol 57: 1247–1261

Noda H, Suzuki DA (1979) The role of the flocculus of the monkey in saccadic eye movements. J Physiol Lond 294: 317–334

Noda H, Sugita S, Ikeda Y (1990) Afferent and efferent connections of the oculomotor region of the fastigial nucleus in the macaque monkey. J Comp Neurol 302: 340–348

Ohtsuka K, Noda H (1991) The effect of microstimulation of the oculomotor vermis on discharges of fastigial neurons and visually-directed saccades in macaques. Neurosci Res 10: 290–295

Optican LM, Robinson DA (1980) Cerebellar-dependendent adaptive control of primate saccadic system. J Neurophysiol 44: 1058–1076

Precht W, Simpson JI, Llinas R (1976) Responses of Purkinje cells in rabbit nodulus and uvula to natural vestibular and visual stimuli. Pflugers Arch 367: 1–6

Rashbass C (1961) The relationship between saccadic and smooth tracking eye movements. J Physiol (Lond) 159: 326–338

Richmond BJ, Optican LM, Podell M, Spitzer H (1987) Temporal encoding of two-dimensional patterns by single units in primate inferior temporal cortex. I. Response characteristics. J Neurophysiol 57: 132–146

Stone LS, Lisberger SG (1990) Visual responses of Purkinje cells in the cerebellar flocculus during smooth-pursuit eye movements in monkeys. I. Simple spikes. J Neurophysiol 63: 1241–1261

Suzuki DA, Keller EL (1988a) The role of the middle vermis of monkey cerebellum in smooth-pursuit eye movement control. I. Eye and head movement-related activity. J Neurophysiol 59: 1–18

Suzuki DA , Keller EL (1988b) The role of the middle vermis of monkey cerebellum in smooth-pursuit eye movement control. II. Target velocity-related Purkinje cell activity. J Neurophysiol 59: 19–40

Suzuki DA, May JG, Keller EL, Yee RD (1990) Visual motion response properties of neurons in the dorsolateral pontine nucleus of the alert monkey. J Neurophysiol 63: 37–59

Thier P, Koehler W, Buettner UW (1988) Neuronal activity in the dorsolateral pontine nucleus of the alert monkey modulated by visual stimuli and eye movements. Exp Brain Res 70: 496–512

Voogd J, Bigaré F (1980) Topographical distribution of olivary and cortico nuclear fibers in the cerebellum: a review. In: Courville J, Montigny C de, Lamarre Y (eds) The inferior olivary nucleus. Raven, New York, pp 207–234

Waespe W, Henn V (1977) Neuronal activity in the vestibular nuclei of the alert monkey during vestibular and optokinetic stimulation. Exp Brain Res 27: 523–538

Waespe W, Cohen B, Raphan T (1985) Dynamic modification of the vestibulo-ocular reflex by the nodulus and uvula. Science 228: 199–202

Zee DS (1982) Ocular motor control: the cerebellum. In: Lesself S, Dalen JTW van (eds) Neuro-ophthalmology. Excerpta Med, Amsterdam, pp 136–147

Zee DS, Yamazaki A, Butler PH, Gucer G (1981) Effect of ablation of flocculus and parafloccullus on eye movement in primate. J Neurophysiol 46: 878–899